

**COHERENT STRUCTURES AND CHAOS: A MODEL PROBLEM**

L. SIROVICH and J.D. RODRIGUEZ

*Division of Applied Mathematics, Brown University, Providence, RI 02912, USA*

Received 18 August 1986; accepted for publication 26 November 1986

The Ginzburg–Landau equation is examined in the chaotic regime. A complete set of uncorrelated coherent structures is extracted from this motion and used as a basis for the dynamical description of coherent structures in the attractor set. The reduced system is shown to describe motions over a wide parameter set.

The aim of this investigation is (1) to isolate the coherent structures of a chaotic motion and (2) to use the coherent structures as a basis set in a dynamical description of the corresponding attractor set. For this purpose we consider the Ginzburg–Landau equation [1] under periodic boundary conditions. This equation, which is of wide current interest [2–5], is known to give rise to chaotic motions [6–9]. In particular we focus on the numerical experiments of Keefe [8].

Consider spatially periodic motions in a box of length  $2\pi$ , governed by

$$G(A) = i\partial A/\partial t + q^2(1 - ic_0)\partial^2 A/\partial x^2 - i\rho A + (1 + i\rho)|A|^2 A = 0. \tag{1}$$

The coefficient  $q^2$  of the diffusion term is easily absorbed in the space variable in which case the box has length  $2\pi/q$ . In the form written, (1),  $q^2$  plays the role of a reciprocal Reynolds number and for this reason is expressed in this way. In the numerical experiments of Moon et al. [7] and Keefe [8] the constants  $\rho$  and  $c_0$  are taken to be  $1/4$  (unless otherwise stated our calculations also adopt these values), and (1) is solved subject to the initial data

$$A = 1 + 0.02 \cos x. \tag{2}$$

Eq. (1) has  $\exp(it)$  as a base solution. This solution, known as the Stokes solution, is known to be unstable [2–4] as  $q^2$  is decreased beyond the critical value. The equation then supports a spatially peri-

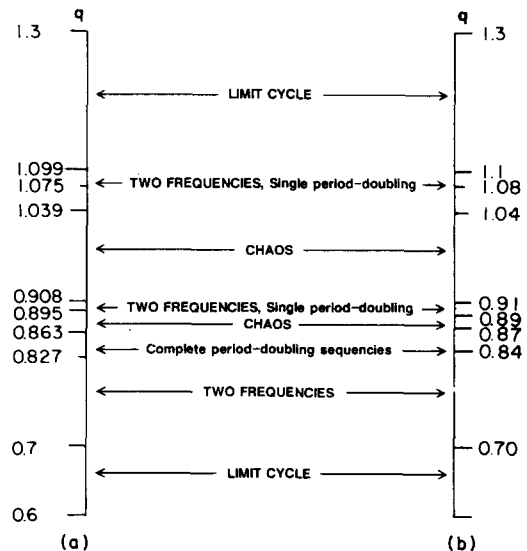


Fig. 1. (a) Summary of qualitative behavior versus  $q$  for Ginzburg–Landau equation. Redrawn from ref. [8]. (b) Same as (a) using the 3-mode approximation.

odic limit cycle, which also becomes unstable as  $q^2$  is further decreased. Next two-torus motion takes place and as  $q^2$  continues to decrease chaos sets in. Fig. 1a is the plot given by Keefe which summarizes the events which take place as  $q$  is varied.

The most chaotic case found by Keefe [8] occurs for  $q = 0.95$ . (The Lyapunov dimension of the attractor attains a maximum of  $\sim 3.05$  for this value of  $q$ .) In this instance three Lyapunov exponents are positive and the fractal dimension of the attractor is 3.05

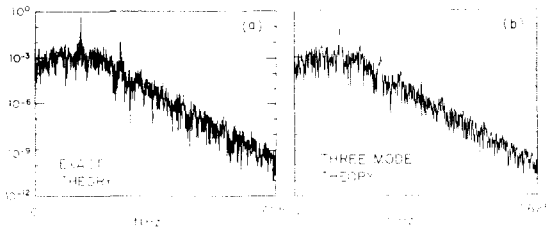


Fig. 2. (a) Power spectrum at  $x=0$  for the Ginzburg–Landau solution at  $q=0.95$ . From ref. [8]. (b) Same as (a) using the 3-mode approximation.

(based on the Lyapunov dimension). In fig. 2a we see the power spectrum, at  $x=0$ , and in fig. 3a a Poincaré section, as found by Keefe [8] for this case.

To consider the problem posed by (1) and (2) one may represent  $A$  as a Fourier series

$$A = \sum A_n(t) \exp(inx) \quad (3)$$

and this in fact lies at the heart of the spectral method used in refs. [7,8] to solve (1). The set  $\{\exp(inx)\}$  is not the only set of orthogonal periodic functions on the interval. More generally we can consider the set  $\{V_n\}$  defined by

$$V_n(x) = \sum \alpha_{nm} \exp(imx). \quad (4)$$

These are orthonormal under the requirement that

$$\sum_k \bar{\alpha}_{ik} \alpha_{jk} = \delta_{ij}. \quad (5)$$

In terms of the set  $\{V_n\}$  we can formally represent  $A$  by

$$A = \sum_{n=1} B_n(t) V_n(x). \quad (6)$$

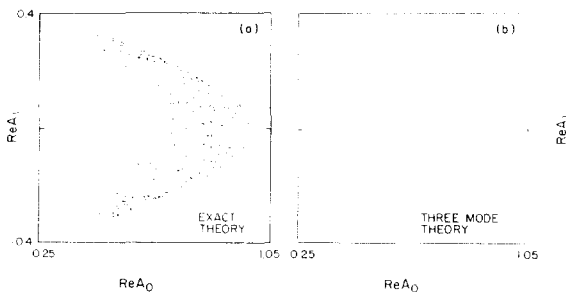


Fig. 3. (a) Poincaré section of the Ginzburg–Landau solution of  $q=0.95$ :  $\text{Re } A_0$  versus  $\text{Re } A_1$ ; taken when  $\text{Im } A_0=0$ , and  $\partial A/\partial x > 0$ . (b) Same as (a) using the 3-mode approximation.

Symmetry considerations imply that the ensemble average of  $A$  vanishes

$$\langle A \rangle = 0. \quad (7)$$

However there is no a priori reason for the coefficients  $\{A_n\}$  in (3) to be uncorrelated. To fix the coefficients  $\{\alpha_{ij}\}$  we require that the coefficients  $\{B_n\}$  be uncorrelated:

$$\langle B_n \bar{B}_m \rangle = \delta_{nm} \lambda_n. \quad (8)$$

From this it follows that

$$\begin{aligned} K(x, y) &= \langle A(x, t) \bar{A}(y, t) \rangle \\ &= \sum \lambda_n V_n(x) \bar{V}_n(y). \end{aligned} \quad (9)$$

Note that  $K(x, y)$  is the two-point correlation function. Viewed in its own right  $K(x, y)$  is a hermitian non-negative kernel. The set  $\{V_n\}$  are clearly the orthonormal eigenfunctions of  $K$ , while the expansion in (9) is a statement of Mercer's theorem [10]. In the statistical literature this is referred to as the Karhunen–Loeve expansion [11]. Lumley [12,13] introduced this expansion in turbulence theory, by suggesting that it be used to determine coherent structures in a turbulent flow.

To implement this procedure we introduce (3) into (9) to get

$$\begin{aligned} K &= \sum_{m,n} \langle A_m \bar{A}_n \rangle \exp[i(mx - ny)] \\ &= \sum_{m,n} M_{m,n} \exp[i(mx - ny)]. \end{aligned} \quad (10)$$

If a typical eigenfunction is represented by

$$V = \sum \alpha_n \exp(inx), \quad (11)$$

then the eigenfunction problem is reduced to the matrix problem,

$$\mathbf{M}\alpha = \lambda\alpha, \quad (12)$$

where  $\lambda$  is the corresponding typical eigenvalue. In the actual calculation we use a 16-point collocation method, and hence integrated 32 ordinary differential equations. (Although this is well below the 64-point collocation method used in refs. [7,8] we are still able to capture the essential features.) We assume ergodicity and replace ensemble averages by time averages. Eq. (1) was then integrated for  $q=0.95$  and the correlation matrix  $\mathbf{M}$  determined. The first six

Table 1

$j$	$\lambda_j$
1	0.5328
2	$0.8548 \times 10^{-1}$
3	$0.1306 \times 10^{-2}$
4	$0.1225 \times 10^{-4}$
5	$0.1835 \times 10^{-6}$
6	$0.2358 \times 10^{-8}$

eigenvalues are shown in table 1. All the rest are  $O(10^{-10})$  or smaller. Due to space considerations we only show the eigenvector corresponding to  $\lambda_1$ . This is given in table 2. Odd components vanish, a fact which follows from symmetry considerations. Fig. 4 contains plots of the real and imaginary parts of the first three eigenfunctions or coherent structures. Since the turbulence or chaos level is relatively low the coherent structures are nearly sinusoidal.

The eigenvalues  $\lambda_n$  can be interpreted as being the average energy in the mode  $V_n$  or alternately as a measure of the time spent by  $A$  in the  $V_n$  direction. In either event we see that only the first few eigenfunctions are significant. With this in mind, we use the set  $\{V_n\}$  in a Galerkin procedure. Specially we truncate at some  $N$  and then project onto the corresponding subspace,

$$\left( V_m, G \left( \sum_{n=1}^N B_n(t) V_n \right) \right) = 0,$$

$$m = 1, \dots, N. \tag{13}$$

The resulting set of  $N$  complex ordinary differential equations can then be integrated in time. In view of the values shown in table 1 we have taken  $N=3$ . Space restrictions forbid us from specifically writing these three equations. Fig. 3b, however, shows the Poin-

Table 2

$k$	Re $\alpha_{1k}$	Im $\alpha_{1k}$
0	0.999	0
$\pm 2$	$0.215 \times 10^{-1}$	$0.200 \times 10^{-1}$
$\pm 4$	$0.458 \times 10^{-3}$	$0.707 \times 10^{-3}$
$\pm 6$	$0.117 \times 10^{-4}$	$0.260 \times 10^{-4}$
8	$0.654 \times 10^{-6}$	$0.198 \times 10^{-5}$

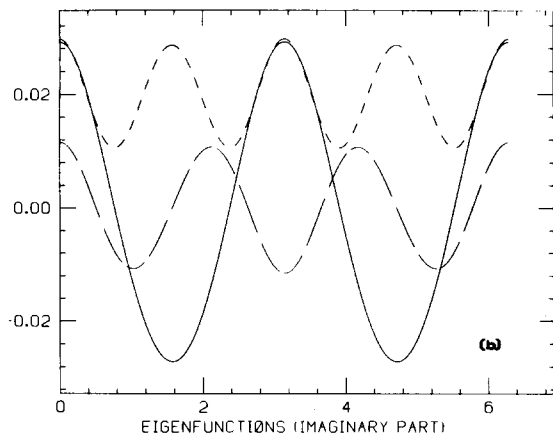
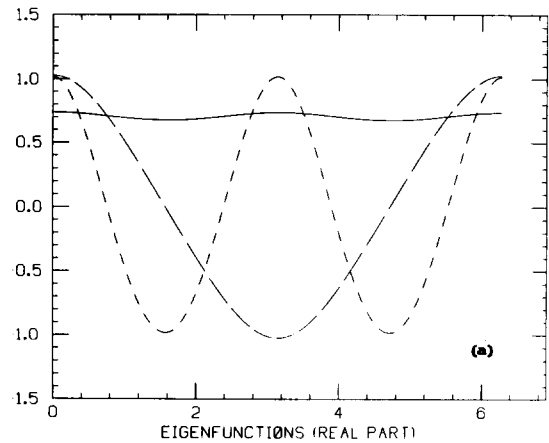


Fig. 4. The complex eigenfunction  $V_n$  for  $n=1$  (continuous),  $n=2$  (long dash),  $n=3$  (short dash). (a) contains the real parts and (b) the imaginary parts.

caré section which results from this integration while fig. 2b shows the corresponding power spectrum. From comparison with the exact integration we must regard the approximation as quite good. In each instance the plots fall neatly over one another. (That 3b appears fatter than 3a must be regarded as an optical illusion.)

We next address the issue of how good is the approximation at values of  $q$  other than the special value of  $q=0.95$  under which the approximation was derived. Fig. 1b contains a summary of the result of using the three complex equations derived for  $q=0.95$  to describe the evolution of the initial data at other values of  $q$ . As a comparison of fig. 1a and fig. 1b

shows the approximation does a remarkably good job. To use the Reynolds number analogy once again, coherent structures determined at one Reynolds number give a good description over a wide range of other Reynolds numbers. As a cautionary remark we observe that a coherent structure calculated at one value of  $q$  is not necessarily a coherent structure at other values of  $q$ . For, at other values of  $q$  the coefficients, in general, become correlated. This is a minor problem since uncorrelated structures can then be obtained from the approximate theory directly.

A seemingly important aspect of the algorithm presented is the fact that relatively few harmonics are excited in the motion. To be specific the equivalent of eight harmonics were considered and hence the calculation was reduced to calculating eigenvectors and eigenvalues of a  $16 \times 16$  hermitian matrix. If the number of harmonics considered is increased by two orders of magnitude this procedure would exceed present machine limitations. We remark in brief that if this is the case an alternative approach is available. Of basic importance is the dimension of the attractor, say  $N$ . Then under various smoothness requirements Whitney's theorem [14] states that the attractor can be embedded into  $R^{2N+1}$ . Of course,  $2N+1$  dimensions are sufficient but not necessary for the embedding space. In the present instance, a dimension of six rather than seven seems to be sufficient. Whitney's theorem lies at the basis of Takens

[15] embedding method and can be employed in the above as an alternate procedure to determine the coherent structures. This will be pursued further at another time.

## References

- [1] V.L. Ginzburg and L.D. Landau, Zh. Eksp. Teor. Fiz. 20 (1950).
- [2] A.C. Newell and J.A. Whitehead, J. Fluid Mech. (1969) 279.
- [3] K. Stewartson and J.T. Stuart, J. Fluid Mech. (1971) 529.
- [4] L. Sirovich and P.K. Newton, in: Problems of non-linear stability, eds. Y. Houssani and R. Voight (Springer, Berlin, 1986).
- [5] L. Sirovich and P.K. Newton, Physica D, to be published.
- [6] Y. Kuramoto, Prog. Theor. Phys. Suppl. 64 (1978) 346.
- [7] H.T. Moon, P. Huerre and L.G. Redekopp, Physica D 7 (1983) 135.
- [8] L. Keefe, Stud. Appl. Math. 73 (1985) 91.
- [9] C.S. Bretherton and E.A. Spiegel, Phys. Lett. A 96 (1983) 3.
- [10] F. Riesz and B.Sz. Nagy, Functional analysis (1955).
- [11] R.B. Ash and M.F. Gardner, Topics in stochastic processes (Academic Press, New York, 1975).
- [12] J.L. Lumley, in: Atmospheric turbulence and radio wave propagation (Nauka, Moscow, 1967).
- [13] J.L. Lumley, Stochastic tools in turbulence (Academic Press, New York, 1970).
- [14] H. Whitney, Ann. Math. 37 (1936) 645.
- [15] F. Takens, Lecture notes in mathematics, Vol. 366, eds. D. Rand and L.S. Young (Springer, Berlin, 1981) p. 366.